

# Semantic scene descriptions as an objective of human vision

Adrien Doerig<sup>1,2</sup>, Tim C Kietzmann<sup>1,2</sup>, Emily Allen<sup>3,4</sup>, Yihan Wu<sup>5</sup>,  
Thomas Naselaris<sup>6</sup>, Kendrick Kay<sup>3</sup>, & Ian Charest<sup>7,8</sup>

<sup>1</sup>Donders Institute for Brain, Cognition & Behaviour, Nijmegen, the Netherlands

<sup>2</sup>Institute of Cognitive Science, University of Osnabrück, Germany

<sup>3</sup>Center for Magnetic Resonance Research (CMRR), Department of Radiology, University of Minnesota, Minneapolis, MN, USA.

<sup>4</sup>Department of Psychology, University of Minnesota, Minneapolis, MN, USA

<sup>5</sup>Graduate Program in Cognitive Science, University of Minnesota, Minneapolis, MN, USA.

<sup>6</sup>Department of Neuroscience, University of Minnesota, Minneapolis, MN, USA.

<sup>7</sup>cerebrUM, Département de Psychologie, Université de Montréal, Montréal, Canada

<sup>8</sup>Center for Human Brain Health, School of Psychology, University of Birmingham, Birmingham, United Kingdom

Interpreting the meaning of a visual scene requires not only identification of its constituent objects, but also a rich semantic characterization of object interrelations. Here, we study the neural mechanisms underlying visuo-semantic transformations by applying modern computational techniques to a large-scale 7T fMRI dataset of human brain responses elicited by complex natural scenes. Using semantic embeddings obtained by applying linguistic deep learning models to human-generated scene descriptions, we identify a widely distributed network of brain regions that encode semantic scene descriptions. Importantly, these semantic embeddings better explain activity in these regions than traditional object category labels. In addition, they are effective predictors of activity despite the fact that the participants did not actively engage in a semantic task, suggesting that visuo-semantic transformations are a default mode of vision. In support of this view, we then show that highly accurate reconstructions of scene captions can be directly linearly decoded from patterns of brain activity. Finally, a recurrent convolutional neural network trained on semantic embeddings further outperforms semantic embeddings in predicting brain activity, providing a mechanistic model of the brain's visuo-semantic transformations. Together, these experimental and computational results suggest that transforming visual input into rich semantic scene descriptions may be a central objective of the visual system, and that focusing efforts on this new objective may lead to improved models of visual information processing in the human brain.

## Introduction

The visual system extracts meaning from retinal inputs and computes representations rich enough to guide actions, inform world models, and allow verbal communication. Classic accounts suggest a functional segregation of the visual system in two distinct cortical pathways <sup>1–3</sup>: a dorsal stream specialised for spatial information (“where”) and a ventral stream specialised for content information (“what”). An influential and widely accepted view is that one of the main objectives of the visual system is to categorise objects <sup>4–6</sup> in a way that is robust to variations in viewing conditions <sup>7–9</sup>.

Neuroscientific studies investigating high-level vision often use stimuli consisting of isolated objects from many categories (e.g. <sup>10–12</sup>), isolated objects presented on textured backgrounds to control for low-level properties (e.g. <sup>13</sup>), or selected natural scenes where objects occupy the majority of the visual field <sup>14–17</sup>. This focus on object representations has contributed to significant progress in understanding the functional organisation of the visual system, showing principled spatial <sup>18–20</sup> and representational <sup>12,16</sup> organisation. In addition, focused efforts using object category labels have driven substantial progress in artificial intelligence <sup>21,22</sup> and computational neuroscience <sup>23–25</sup>, where category-trained deep neural network (DNN) models currently provide the best predictive performance for activity levels measured in visual ventral stream <sup>26–31</sup>.

Despite this substantial progress, it is not clear whether the characterization of the visual ventral stream as an object processor adequately captures how the brain processes complex naturalistic scenes. From a theoretical standpoint, it is clear that visual scenes convey more information than just the identity of the objects in the scenes <sup>32</sup>. For successful behaviour, a visual organism must understand entities in the world and their ongoing interactions <sup>33</sup>. Presumably, an evolutionarily fit organism must be able to place objects, their context, and their relations together into a coherent interpretation of the scene’s semantics. Moreover, this must be done in such a way that visual information is transformed into representations that can be integrated with other brain systems and communicated with other individuals through language.

One might object that language-related characterizations have no place in describing how the visual system works—in short, language and vision are two distinct brain functions. On the contrary, we believe that a reasonable framework for visual neuroscience casts visually-derived information on a continuum ranging from “low-level” properties (e.g. oriented edges), through “mid-level” properties (e.g. textural information) and “high-level” properties (e.g. object category), to “higher-level” properties (e.g. semantic scene descriptions), all of which can be precisely operationalised and objectively studied (Figure 1). Note that we use the term ‘semantic scene description’ to refer to rich information about scenes, including which objects are present, how they relate to each other in space and semantically, and how the meaning of a scene relates to that of other scenes. Hence, semantic scene descriptions subsume, and go beyond, a simple enumeration of the object categories in an image. They also go beyond embedding each category separately in a semantic space, such as using embedding techniques to determine that “dog” is closer to “cat” than to “french fries” <sup>34,35</sup>. Rather, semantic scene descriptions are computed at the whole-sentence level <sup>36–38</sup>.

In this paper, we use a large-scale 7T fMRI dataset of responses to complex natural scenes <sup>39</sup> to investigate the extent to which object labelings are sufficient for describing visual representations, or alternatively, whether semantic scene descriptions might provide better characterization of visually evoked activity. We also provide a model of how the transformation from retinal inputs into semantic

representations might be achieved by the brain. Our results suggest that the overarching function of visual processing might be to compute scene descriptions, and not merely object labels.

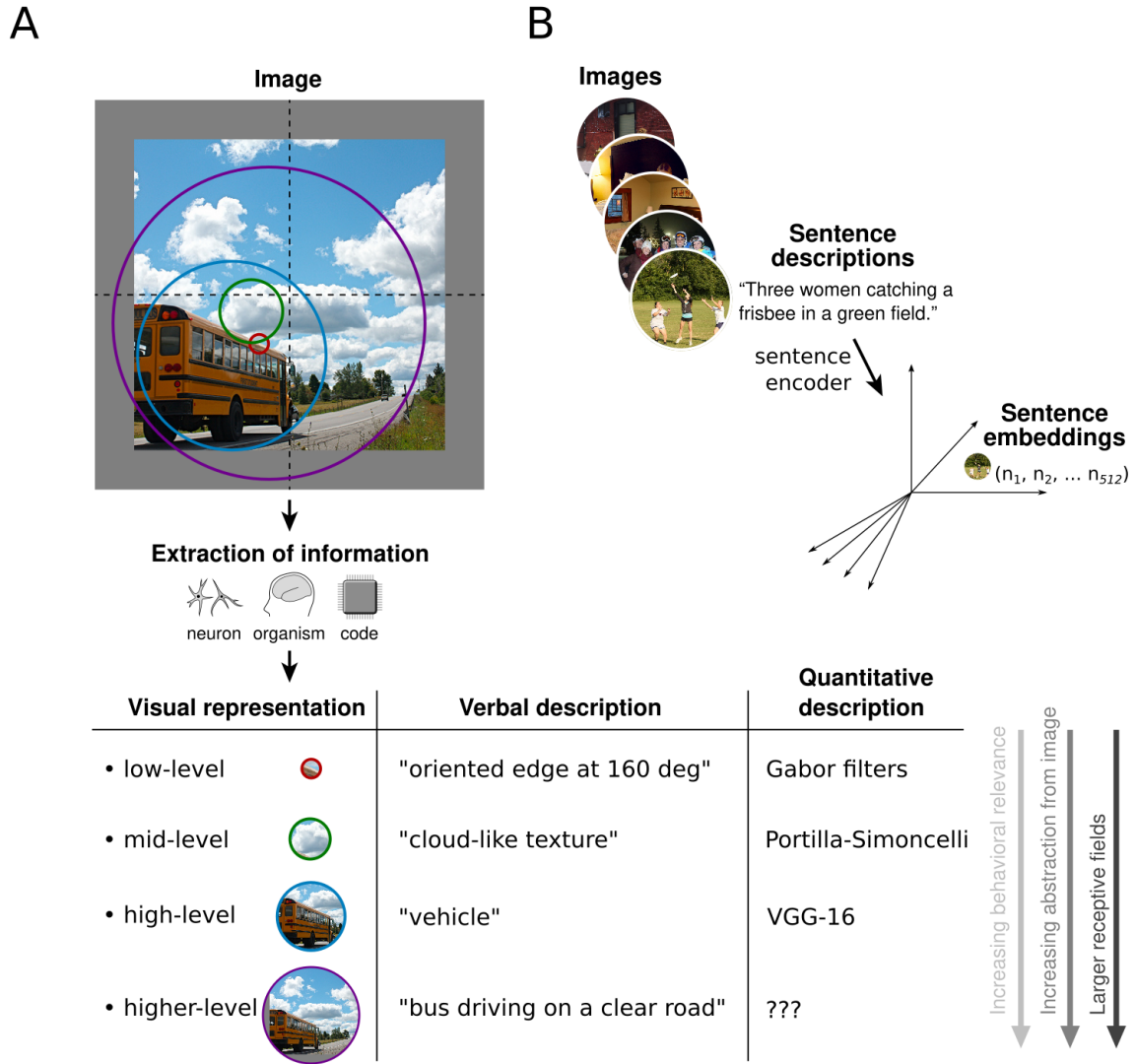


**Figure 1. A framework for understanding semantics in visual neuroscience. A. Visual representations.** Properties of a visual image can be extracted to form visual representations. This extraction can be instantiated in the activity of a neuron (or brain area), performed consciously by an organism, or achieved by code implementing specific operations. In visual neuroscience, it is conventionally believed that visual processing forms a hierarchy from early, low-level representations to late, high-level representations. As the hierarchy is ascended, receptive fields generally increase in size, features become increasingly abstract relative to the original image, and representations become more behaviorally relevant. In this context, *semantic scene descriptions* are simply higher-level representations. At all levels, both verbal and quantitative descriptions of representation are achievable<sup>22,40,41</sup>. **B. How scene descriptions are operationalized.** Each image is associated with several captions written by different human observers to describe the scene. These captions are passed through the GUSE neural network<sup>36</sup> to generate semantic embeddings in a 512-dimensional space.

## Results

To explore visuo-semantic transformations in the human brain, we take advantage of the recent Natural Scenes Dataset (NSD), a large-scale 7T fMRI dataset in which tens of thousands of responses to complex natural scenes were measured in eight individuals<sup>39</sup>. Importantly, the scenes were taken from the COCO image database<sup>42,43</sup> which includes human-provided sentence captions describing each image. Using the Google Universal Sentence Encoder (GUSE), a deep neural network that generates 512-dimensional embeddings from text<sup>36</sup>, we projected each COCO scene description into a 'semantic embedding' space to characterise the semantic content of the visual scene.

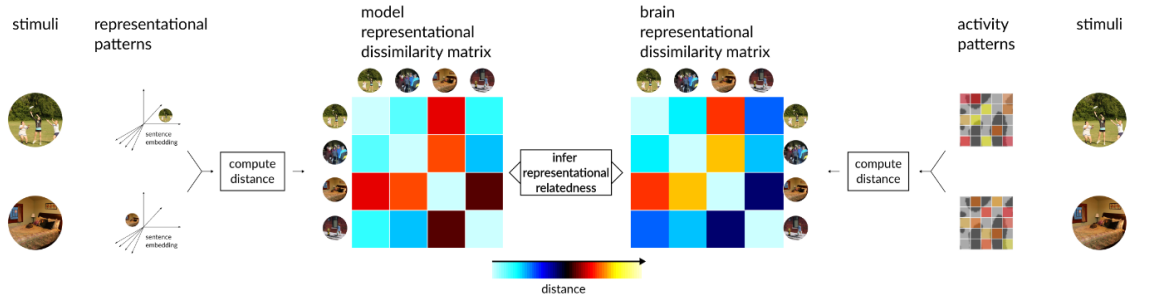
### *Semantic embedding of image captions better explain brain activity than categories*

First, we compared how well semantic embeddings of natural scenes explain brain activity using a representational similarity analysis (RSA;<sup>12,44–46</sup>) searchlight approach (Figure 2A). In this approach, we construct semantic RDMs reflecting the sentence embeddings, brain-activity RDMs from small local groups of voxels (searchlight) based on their responses to the NSD images, and then construct maps indicating where the model RDMs correlate with the brain RDMs. This analysis reveals a set of brain areas whose representational space significantly correlates with semantic space, including but not limited to the visual ventral stream (Figure 2B).

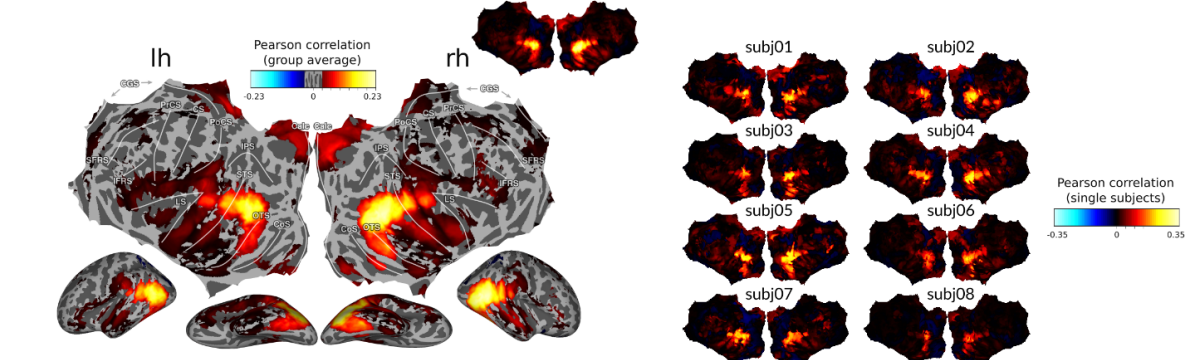
To assess how well categories, as opposed to semantics, can explain the brain data, we conducted the same analysis using multi-hot vectors that encode each image as a "bag of categories", but leave out other semantic meaning and relationships between these categories. The searchlight procedure using this category representation highlights a smaller set of brain regions whose representational space significantly correlates with category space, including lateral occipital complex (LOC; Figure 2C). A quantitative comparison of the searchlight maps for semantic and category RDMs reveals that semantic space captures brain representations significantly better than category space across a widespread network of brain regions, including LOC and early visual areas (Figure 2D).

In summary, we have identified a widespread network of brain regions in which brain activity is better explained by semantic rather than category information. This semantic network includes regions classically linked to semantic processing, such as regions of the anterior temporal lobe, but also early visual areas, down to V1, suggesting that the entire visual system may be geared, to some degree, towards semantic, rather than category, representations. Remarkably, this cannot be explained by the fact that subjects were actively performing a semantic or captioning task. Rather, in the NSD dataset, subjects were performing a continuous recognition task in which they attempted to determine whether the presented image had been shown previously. We thus conclude that the brain automatically translates visual inputs into a semantic format by default, even in the absence of a semantic task.

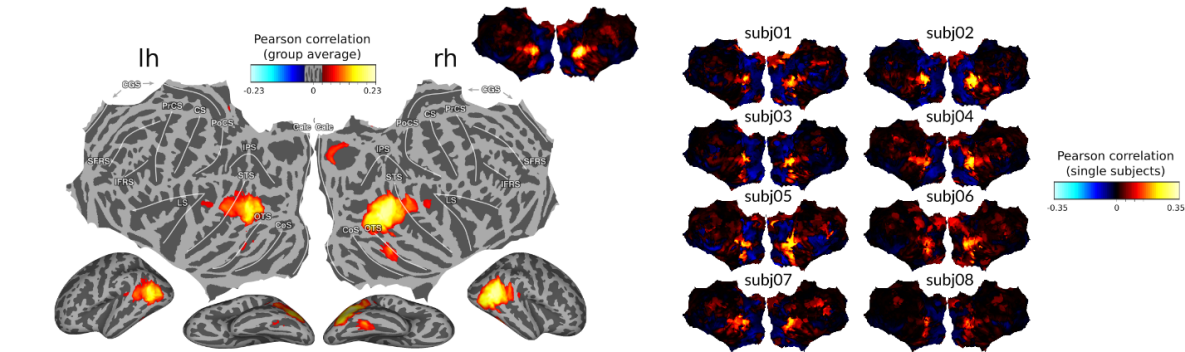
### A Inferring model and brain representational relatedness



### B Mapping semantic representations in the brain



### C Mapping category representations in the brain



### D Model differences

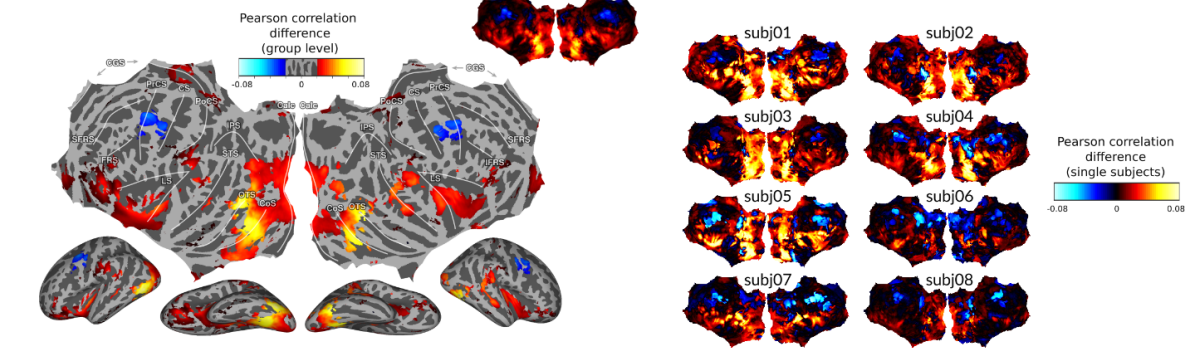


**Figure 2. Semantic representations provide a better characterization of visual representations measured by 7T fMRI. A. RSA approach.** The relatedness of a given model space and the brain's representational space is quantified by computing the Pearson correlation between RDMs constructed from model features and RDMs

constructed from voxel activity patterns. **B. Semantic maps.** Searchlight map for the correlation between semantic space (as given by GUSE embeddings) and brain representational space. *Left:* Group average. *Right:* Individual participants. **C. Category maps.** Searchlight map for the correlation between category space (as given by multi-hot vectors) and brain representational space. *Left:* Group average. *Right:* Individual participants. **D. Difference between semantic and category searchlight maps.** *Left:* Group average. *Right:* Individual participants. Overall, semantics explain brain representations better than categories across a large semantic network.

#### *Scene descriptions can be decoded from brain activities*

To test the robustness of the link between semantics and brain activity, we applied a simple algorithm to decode semantic embeddings from fMRI data and predict sentence captions for brain activity patterns in response to novel natural scenes. Specifically, we learned a linear mapping from cortical activity to predicted GUSE semantic embeddings (Figure 3A, step 1), relying on regularisation to appropriately weigh different brain regions. We then used a separate test set (not used for training the mapping) to evaluate the quality of the decoding. For each given image, we took the measured brain activity and used the trained mapping to generate a predicted semantic embedding (Figure 3A, step 2). To generate a human-interpretable sentence, we used a simple "dictionary" lookup scheme<sup>47</sup> to find the sentence from a large corpus of 3.1 million sentence candidates whose GUSE embedding is closest to the GUSE embedding predicted from brain activity (Figure 3A, step 3).

We find that this approach produces remarkably accurate descriptions of the images viewed by participants, based only on a linear transform of brain activity (Figure 3B). Importantly, from a machine learning perspective, producing semantic scene descriptions from image data is a difficult task that usually requires complex, non-linear transformations<sup>48,49</sup>. Hence, the high performance of our simple linear decoder indicates that the brain performs complex, non-linear operations that generate semantic scene descriptions and that we are able to measure and interpret this information effectively. In addition, this linear mapping from brain activity to semantic embeddings can also be inverted: using the semantic embeddings as an encoding model to predict fMRI voxel-wise responses highlights similar brain regions as the above searchlight analysis (see Supplementary Figure 1), providing converging evidence for a widespread semantic network devoted to representing semantic scene descriptions.

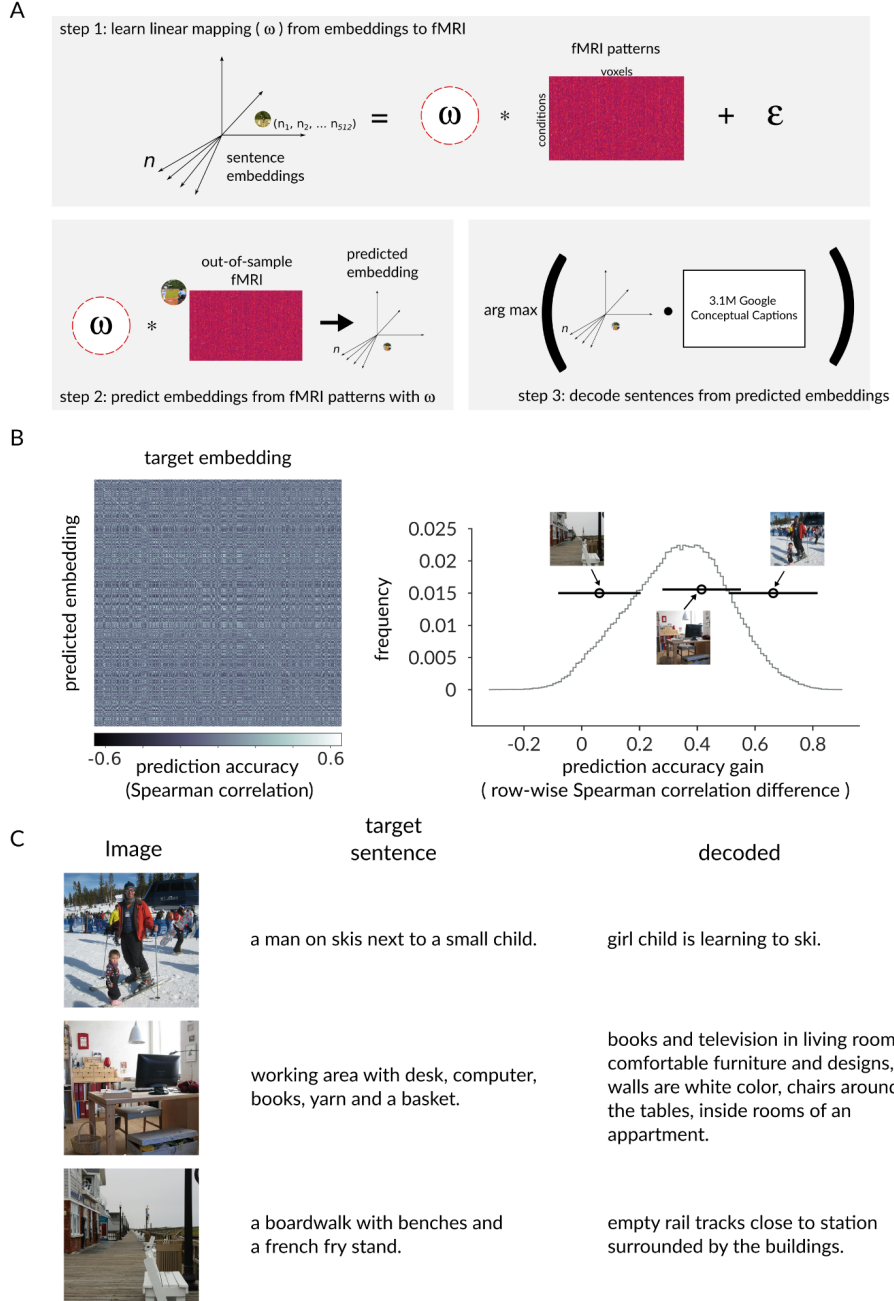


**Figure 3. Whole brain fMRI brain reading.** A simple linear nearest neighbour decoding approach achieves good reconstruction of full sentences, based on whole brain data. **A. Decoding method.** *Step 1:* A linear mapping from whole brain activity to GUSE embedding space is learned through cross-validated ridge regression on a train set. *Step 2:* This decoder is applied to held-out fMRI activities, to predict the corresponding GUSE embedding of the scene description. *Step 3:* A nearest neighbour approach is used on 3.1 million image captions to find the sentence in GUSE embedding space closest to the predicted GUSE embedding. This nearest neighbour sentence is used as a human-interpretable output of our decoder. **B. Decoding performance.** *Left:* Correlation matrix between predicted and target embeddings. *Right:* Prediction accuracy gain histogram. For each image, the mean correlation between the predicted embedding and the true embeddings of other images (off-diagonal in the correlation matrix) is subtracted from the correlation between the predicted embedding and the target embedding (diagonal in the correlation matrix). Hence, higher values show better decoding performance. Dots show the prediction accuracy gain for individual images displayed in panel C. **C. Decoded sentence examples.** From top to bottom: decreasing prediction accuracy gain.

## A Deep Recurrent Convolutional Network trained on semantic scene descriptions

Traditionally, the visual system is conceptualised in terms of category-related computations. In contrast, our results suggest that activities in the visual system are better explained by semantic information. However, this does not yet provide a mechanistic account of how these visuo-semantic computations are performed. We tackled this question by training a deep recurrent convolutional neural network (RCNN) to map input images onto GUSE semantic embeddings on the MS-COCO dataset (note that although the images used in the NSD dataset are part of MS-COCO, they were removed from the training and validations sets here), and testing how different layers and recurrent timesteps explain the fMRI data for the NSD dataset (Figure 4A).

Applying the same RSA and searchlight approach as in experiment 1 to the last layer and timestep of the network revealed a similar semantic network as we had found using GUSE embeddings in experiment 1 across subjects (Figure 4B). In addition, since the network does not perfectly predict GUSE embeddings from its pixel input, we wondered if this departure from purely semantic information reflected a visuo-semantic transition that helped explain brain data. When contrasting GUSE embeddings from experiment 1 and the last time step and layer of our network, we found that our network indeed explains brain data *better* than the GUSE embeddings they were trained towards, over a widespread set of regions that includes (but is not limited to) the semantic network highlighted in experiment 1 (Figure 4C). This shows that these regions are not only semantic, but rather represent the *interplay between visual and semantic information*, which our model can capture mechanistically. Given that the mechanistic path to semantic embeddings seems as important as the embeddings themselves to explain brain data, we explored earlier layers and timesteps. Using non-negative least-squares fitting across layers and timesteps, we found that the network as a whole predicts brain data well throughout the entire visual system, and on to the visuo-semantic network across subjects (Figure 4B inset; see Supplementary Figure 2 for individual subjects).

Such a mechanistic model allows for isolating and testing the impact of semantic training and of recurrence. A control network trained on multi-hot category vectors instead of semantic embeddings also explained activity across many areas, but was outperformed by the semantic model (Supplementary Figure 3A), again suggesting that the visual system is better seen as computing semantic information rather than category information. Interestingly, the semantically trained model outperformed the category-trained model not only in semantic regions, but also in early visual cortex (EVC). To explore the effects of recurrence, we ran a second control network trained on semantics, but with only feedforward connections. We contrasted how well this semantically trained feedforward control predicted brain activity compared to its recurrent counterpart. We found that the feedforward control predicted high-level semantic areas as well as the recurrent network, but was outperformed in EVC (Supplementary Figure 3B). Hence, recurrence seems to improve the fit of the semantic model to EVC. One possible mechanism is that semantically related information is fed back through recurrent connections. To further explore this hypothesis, we compared how well early (layer 1), middle (layer 5), and late (layer 10) layers explain data during the feedforward sweep (timestep 1) and at the end of recurrent processing (timestep 6) of our recurrent network trained on sentence embeddings. We found that recurrence improves EVC predictions over time, especially for lower network layers (Supplementary Figure 3C). These results suggest that semantic information is computed in high-level layers and then fed-back to lower layers, allowing the model to explain

feedback from higher brain regions to EVC.

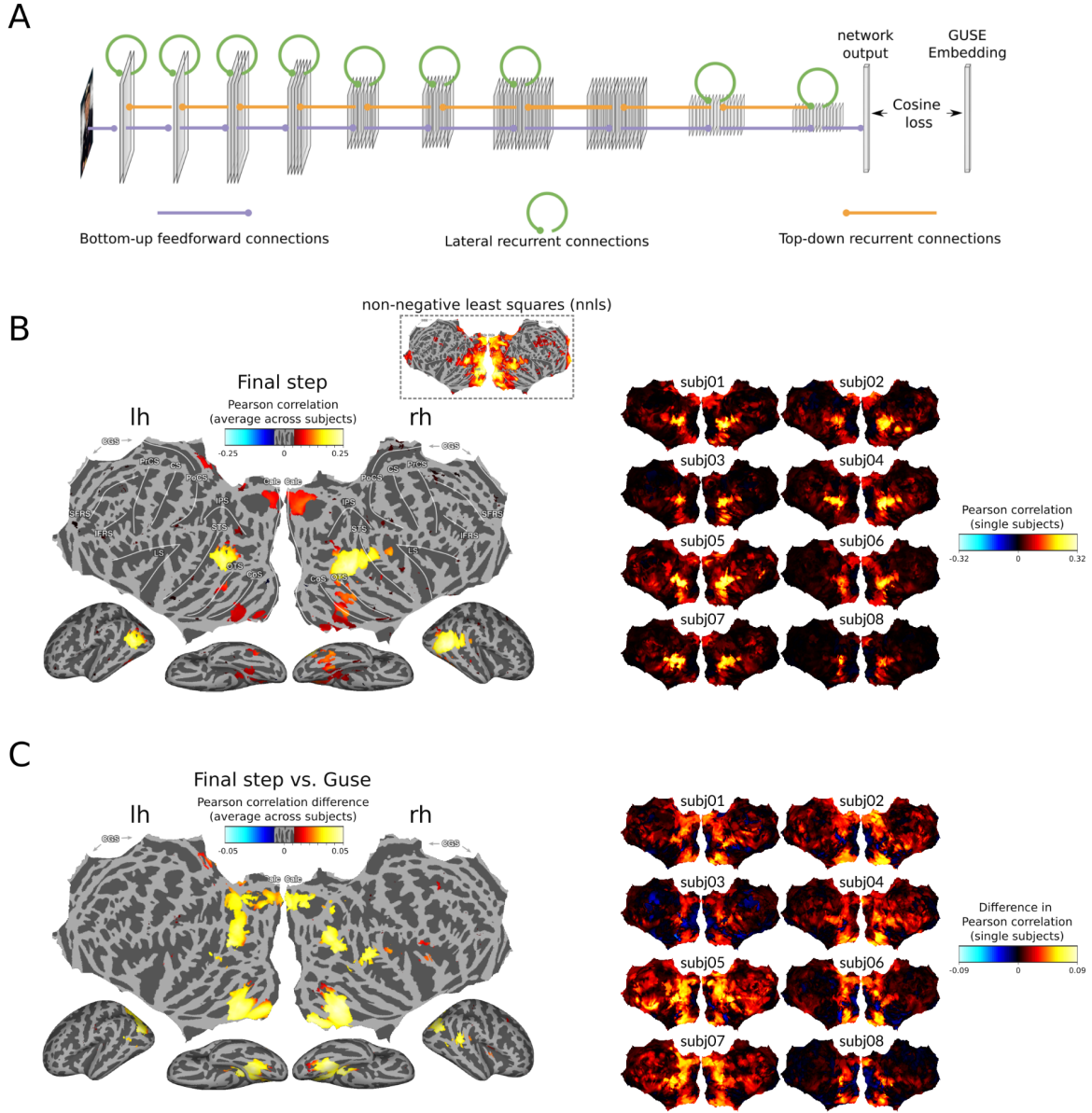


**Figure 4. Deep Recurrent Convolutional Networks. A. Network architecture.** Our RCNN model is based on the vNet architecture, with ten fully recurrent convolutional layers with bottom-up (purple), lateral (green) and top-down (orange) connections, followed by a fully connected readout layer. The receptive field sizes are chosen to be as close as possible to human foveal receptive field sizes<sup>50</sup>. The objective of the network is to minimize the cosine distance between the predicted and the target GUSE semantic embedding. **B. Searchlight RDM maps for RCNN last layer, final timestep.** For each searchlight location, the correlation between the fMRI RDM and network last layer & timestep RDM is shown. Results highlight a similar semantic network as found in experiment 1. *Left:* Across subjects. *Right:* Individual subjects. *Inset:* Cross-validated non-negative least squares fit of the whole network, showing that the network as a whole can explain neural data across the visual system, and on to the semantic network. **C. Contrast between RCNN and GUSE maps.** *Left:* Across subjects. *Right:* Individual subjects. The last layer and timestep of the recurrent network explains neural data better than GUSE semantic embeddings over a wide array of regions, showing that these regions are not purely semantic, but rather reflect visuo-semantic computations.

## Discussion

Using a variety of converging analysis approaches on a large-scale visual neuroimaging dataset, we have provided evidence that visually evoked responses in the brain can be viewed as a translation of visual inputs into semantic representations. These representations, importantly, are richer than object categories, which have been the traditional focus of cognitive neuroscience. While categories are likely an important component of the goal of visual processing<sup>51</sup>, we have shown that there is additional information in the neuroimaging data. The crucial contribution of semantics likely consists in relationships between the different objects in a scene, described in language as verbs and prepositions (such as “A tiger *running towards* you), or adjective-modified nouns (“A *sleepy* tiger”). We suggest that extracting such semantic scene content is reasonable as a default output of visual processing, because such content is behaviourally relevant and critical for communication with the rest of the brain, and with other individuals. A challenge for future work is better understanding the precise format of the brain’s semantic representations. Here, we used GUSE embeddings to operationalize semantics, but there are other possibilities, such as sentence embeddings derived from other models, or visuo-semantic embeddings derived from recent multimodal models such as CLIP<sup>52</sup>. Comparing which embeddings best explain brain data, and characterising the structure of these embedding spaces, will provide important information about semantics in the brain<sup>31</sup>.

Crucially, the visuo-semantic transformations that we studied are automatic. Indeed, we found a widespread viso-semantic network of brain areas even though subjects did not perform a semantic task, suggesting that semantic scene description is an important general objective of vision. One consequence of this automaticity where mere exposure to visual input leads to semantic representations is that we can decode semantic content from imaging data surprisingly easily using a linear method (Figure 3). Other groups have applied brain reading methods to decode images<sup>53</sup>, category information<sup>15</sup>, speech<sup>54</sup> and image captions<sup>55</sup> from neuroimaging data, but the models employed were generally much more complex. For example, Huang et al. used a complex dual channel deep network, including CNN and transformer components. In contrast, our approach aims to show that brain representations have *already extracted semantic scene descriptions* that can be decoded using a simple linear readout. In addition, this suggests applications, for example to communicate with patients that cannot use language, where the simplicity of linear readouts may allow for faster, easier to train models compared to more complex methods (and the two approaches can be combined).

Interestingly, the advantage of semantics compared to categories in explaining brain representations extends across the visual system, all the way to early visual areas (although it should be noted that the absolute performance of both are low, see Figure 2D). This may be due to cortical feedback from high-level areas devoted to semantic descriptions, a possibility reinforced by our modelling results showing that early visual cortex is better explained in semantically trained models after recurrent processing. Alternatively, it may suggest that semantic scene descriptions are an important objective of the visual system, which possibly influences feature extraction at the earliest stage of processing. These possibilities are not mutually exclusive, and imaging methods with better temporal resolution, such as MEG, may help resolve this question.

A major open question is how the brain computationally constructs semantic representations from visual inputs. As we have argued, there is no fundamental qualitative difference between low-level

and high-level representations (Figure 1). As a proof-of-concept mechanistic model of this process, we trained a recurrent neural network that transforms visual inputs into semantic embeddings along a hierarchy of layers, culminating in similar representation as in the brain’s semantic network (Figure 4B). Far from a black box, this network sheds further light on visuo-semantic transitions in the brain by showing (i) that semantic objectives better explain brain data than category objectives, providing a normative argument in favour of semantic scene descriptions as an objective of the visual system (Supplementary Figure 3A), (ii) that several brain regions are better characterised as performing *visuo-semantic*, rather than purely semantic, computations (Figure 4C) and (iii) indicating that feedback carries semantic information from higher areas down to early visual cortex (Supplementary Figure 3B&C). This suggests that future efforts in computational neuroscience might fruitfully use semantic embeddings as the cost metric. Machine learning applications may benefit from a shift from categories towards semantic scene descriptions too, as the latter carry richer information about the visual world than the categories which are standardly used to train current systems. This will allow systems to learn more information per training example, and may help create more robust systems with better scene understanding.

Exactly what drives the design and organisation of the visual system remains a broad open theoretical question. Our results suggest that the visual system might have as its objective, presumably through the course of evolution, the construction of semantic scene descriptions. Going forward, it will be critical to test this through quantitative models against other major theories of visual processing such as category untangling<sup>51</sup>, predictive coding<sup>56</sup> and other bayesian approaches<sup>57</sup>, or reverse hierarchy theory<sup>58,59</sup>. One current limitation of investigating scene descriptions is the paucity of high-quality, large-scale datasets of images with human-generated captions. Certain datasets offer large quantities of annotated images (e.g. the Google Conceptual Captions dataset), but these are either automatically generated, or not well controlled, and may not be as relevant as human-generated captions. For this reason, we trained our network on MS-COCO, which is very small by today’s machine learning standards, so larger datasets are very likely to improve model performance.

Foundational previous work also demonstrated widespread areas with semantic representations<sup>60-63</sup>. However, most of these studies focus on semantics alone using spoken language, and not visuo-semantic transitions as studied here. One exception is Popham et al.<sup>64</sup> who showed that semantic and visual selectivities align across a cross-modal boundary, but that study used two different experiments, one visual and another one using spoken language, instead of showing how images are automatically transformed into semantics by the visual system given only visual input. Another exception is Güçlü & Van Gerven<sup>62</sup>, who used single word embeddings to predict visually evoked brain activities on a small dataset, instead of a large-scale exploration of sentences describing scenes. To our knowledge, the present work is the first study leveraging *sentence* embeddings, as opposed to word embeddings, to operationalize semantics in the brain. This is important, since, as mentioned, single words do not convey the meaning of a scene and can instead be seen as performing a refined kind of label smoothing<sup>65</sup>. Hence, our study is the first to show how the brain automatically extracts semantic scene descriptions from images.

Importantly, the present results go beyond previous work contrasting AI engineering models that combine image and text data (such as CLIP transformers) with category-trained visual CNNs<sup>66,67</sup>. Although these studies provide some evidence that semantics can help explain variance in visual

responses, they face important confounds. They contrast representations of a complex transformer architecture with a substantially different visual DNN architecture. In addition, the data used for training are different and not comparable between the two models. Hence, the impact of semantics cannot be disentangled from differences in architectures and training data. Our results overcome these challenges and directly demonstrate the advantage of semantics vs. category information without an intervening model. Furthermore, our RCNN modelling avoids such confounds because our models only differ in the semantic objective, while controlling for both dataset and architecture. Furthermore, our RCNN networks, which highlight the roles of hierarchical depth and feedback, are more realistic models of biological vision, bringing the architecture into closer alignment with the task of modelling brain function. Finally, our comparisons are based on RSA, which, due to the low number of free parameters, provides more definitive model adjudication compared to parameter-rich encoding model approaches<sup>60,68-70</sup>.

An influential theory of semantics in the brain is the hubs and spokes model<sup>71</sup>. According to this theory, the semantic network in the brain consists in modality specific “spokes” that converge on a central amodal “hub” in the anterior temporal lobe (ATL) that integrates information across modalities. In the framework of this theory, our results can be seen as focussing on the visuo-semantic spoke of this network, which may be integrated with other information in the ATL hub. This account would predict correlations between semantic embeddings and the representations in ATL, but the ATL cannot easily be imaged using fMRI, so further studies are needed to clarify this possibility.

If the visual system translates retinal inputs into rich and meaningful semantic representations, this opens up new avenues of research, in particular to elucidate the mechanisms behind visuo-semantic computations, potentially mediated by a visuo-semantic hierarchy as in our models, feedback from amodal regions to the visual system<sup>71</sup>, local crossmodal computations<sup>64</sup>, or other possibilities. The shift in perspective from categories to more meaningful and behaviorally relevant semantic descriptions is finally made possible by recent technological breakthroughs and offers a new and promising framework for progress in visual neuroscience.

## Methods

### *The Natural Scenes Dataset*

A detailed description of the Natural Scenes Dataset (NSD; <http://naturalscenesdataset.org>) is provided in a separate manuscript<sup>39</sup>. This dataset contains measurements of fMRI responses from 8 participants who each viewed 9,000–10,000 distinct colour natural scenes over the course of 30–40 scan sessions, for a total of 73000 images. Scanning was conducted at 7T using whole-brain, gradient-echo EPI at 1.8-mm isotropic resolution and 1.6-s repetition time. Images were taken from the Microsoft Common Objects in Context (COCO) image dataset<sup>42</sup> and were presented for 3 s with 1-s gaps in between images. A special set of 1,000 images were shared across subjects; the remaining images were unique and mutually exclusive across subjects. Subjects fixated centrally and performed a long-term continuous recognition task on the images. The data were pre-processed by performing one temporal interpolation (to correct for slice time differences) and one spatial interpolation (to correct for head motion) and then using a general linear model to estimate single-trial beta weights. In this paper, we used the 1.8-mm volume preparation of the NSD data, beta version 3 (betas\_fithrf\_GLMdenoise\_RR).

### *Characterising the semantic representational space of the natural scenes dataset*

To characterise the semantic representational space of the images shown to the NSD participants, we used representational similarity analysis (RSA; <sup>12,44–46,72</sup>) and embeddings derived from natural language processing. Sentence captions, describing the content of each natural scene, were obtained from five human observers as part of the Microsoft COCO dataset<sup>42,43</sup>. For each NSD participant independently, and for each image presented to the participant, we gathered the five sentence captions provided for that image and took the mean of the resulting embeddings (to account for inter-rater differences). This mean embedding is then passed through the Google Universal Sentence Encoder (GUSE; <sup>36</sup>, a deep neural network generating 512-dimensional embeddings from text. The resulting sentence embedding is a 512 dimensional vector, which is approximately normalised. To create a semantic representational dissimilarity matrix (RDM), for each pair of images presented to the participant, we compute the cosine distance between the pair's embeddings. This results in a 10,000x10,000 RDM which captures the semantic representational space based on the sentence captions. We then compare this semantic RDM against brain RDMs in a searchlight procedure described below.

### *Information-based brain mapping*

Representational dissimilarity matrices were constructed from participants' native space single-trial beta weights using a volumetric searchlight analysis<sup>73,74</sup>. For each voxel  $v$ , we extracted condition-specific activity patterns in a sphere centred at  $v$  with a radius of 5 voxels (searchlight at  $v$ ). Analyses were restricted to images that had been seen three times by the participant, and beta weights were z-scored across single trials within each scanning session for each participant. We then averaged over the condition's three repetitions to get an average response estimate for each experimental condition. For each searchlight  $v$ , the averaged z-scored beta weights were compared between pairs of stimuli using cosine distances to create searchlight RDMs. Given the depth of the NSD dataset, we devised a sampling procedure to relate the brain RDMs to the semantic RDMs. We first randomly sampled 100 conditions from the participant's 10,000 conditions. We indexed the

brain activity patterns for these 100 conditions and constructed the searchlight RDMs for this subset. We also indexed the semantic RDMs to retrieve the pairwise distances related to the sampled conditions. This led to RDMs with an upper-triangular vector length of 4950 pairs in the semantic model, and in the searchlight spheres. These upper-triangular RDMs were then compared between brain and model using Pearson's correlation coefficient, resulting in a volume of Pearson correlations that reveal the correspondence between the brain and model representational geometries. The randomly sampled 100 images were then removed from the condition sampling pool, and we repeated the sampling procedure until we had exhausted all 10,000 conditions. This resulted in 100 correlation volumes (N.B. 4 participants completed the NSD protocol, while another two had seen all three repetitions of 6234 images and 2 participants had seen the three repetitions for 5445 images; leading to 100 splits, 62 splits, or 54 splits depending on the participant), from which we computed parametric t-tests in single participants. These t-volumes allowed assessing the stability of the correlations, and showed highly reliable effects in each participant (with t-values reaching well above 50). Group-level statistics reported in the manuscript are performed using t-tests across the 8 NSD participants, and corrected for multiple comparisons with an alpha of 0.001. Average correlation maps across splits and participants, thresholded with our group-level statistics are then projected in freesurfer's fsaverage surface space, and visualised on a flattened cortical flatmap.

#### *Decoding of semantic features from brain data*

We attempted to reconstruct sentences from brain activity by learning a direct linear mapping from brain activity to the sentence embedding features. This involved a regularised linear regression framework that was solved for each subject separately. In this framework, the modelled data,  $\mathbf{y}$ , consists of the sentence embeddings ( $n$  images  $\times$  512 features) and the predictors,  $\mathbf{X}$ , consists of brain activity measurements ( $n$  images  $\times$   $p$  voxels). For the brain activity measurements, we used betas from the entire cortical surface fsaverage preparation (as described previously).

We set aside a *validation set* to test the performance of the decoding, by holding out the shared 1,000 images. Out of the remaining images, we randomly chose a subset of 1,000 images(?) as a *test set* for hyperparameter evaluation, leaving the remaining images as a *training set*. We used an efficient implementation of ridge regression, termed fractional ridge regression {cite}, to estimate the parameters,  $\mathbf{h\_hat}$  ( $p$  voxels  $\times$  512 features), that represent the optimal sets of weights to apply to the predictors ( $\mathbf{X}$ ) to best predict each of the sentence embedding features ( $\mathbf{y}$ ). Specifically, weights were estimated for 20 different regularisation fractions (0.05 to 1 in increments of 0.05). The cross-validation performance for regularisation fraction was evaluated on the test set. The fraction that best predicted each embedding feature was identified. Finally, the corresponding weights were used to predict the sentence embeddings:  $\mathbf{y\_hat} = \mathbf{X\_validation} * \mathbf{h\_hat}$ , where  $\mathbf{y\_hat}$  is  $v$  images  $\times$  512 features,  $\mathbf{X\_validation}$  is  $v$  images  $\times$   $p$  voxels, and  $\mathbf{h\_hat}$  is  $p$  voxels  $\times$  512 features.

To obtain a sentence reconstruction, we used a simple "dictionary" lookup scheme <sup>47</sup>. We took a large set of 3.1M sentences from Google's conceptual captions (<https://ai.google.com/research/ConceptualCaptions>), embedded these sentences, yielding  $\mathbf{D}$  with dimensionality  $d$  sentences  $\times$  512 features. We then compared these embeddings against the embeddings predicted based on the brain data: for a given image, we computed the distance between each of the  $d$  sentences in the dictionary and the predicted embedding for the image. The

sentences that were closest to the predicted embedding were chosen as the reconstructed sentence (see Fig3).

#### *Recurrent convolutional neural network models*

Our DNN models are derived from *vNet*, a 10-layer convolutional deep neural network architecture designed to closely mirror the progressive increase in foveal receptive field sizes found along the human ventral stream, as estimated via population receptive fields <sup>50</sup>. In contrast to previous instances of *vNet*, our network is recurrent, including both lateral and top-down recurrent connections following a convolutional pattern (Figure 4a), as implemented by Kietzmann et al. <sup>29</sup>.

We used the MS-COCO dataset for training. Since the NSD dataset is based on a subset of MS-COCO, we removed the 73000 images of the NSD dataset from the training and validation sets, and used them as our testing set (i.e., the networks did not see any of the NSD images during training, nor in validation). This resulted in 48236 MS-COCO images for training, 2051 for validation and the 73000 images part of both MS-COCO and NSD for testing.

We trained our recurrent *vNet* to map cross-modally from pixels, i.e. MS-COCO images, to GUSE semantic space. This was possible, because each MS-COCO image has a set of five human-generated captions, which can be mapped into GUSE space as described above. The objective of the network was to minimise the cosine distance between the predicted and the target GUSE embeddings. With this approach, the network transitions from a pixel-based representation to one derived from semantics. As a result, semantically related captions project to nearby locations, whereas sentences that are not related will end up in separate target positions.

To control for the impact of semantic vs. category objectives, we trained a separate *vNet* on a more traditional category objective (i.e. minimising cosine distance using a multi-hot category encoding the categories present in the MS-COCO image). This objective yields networks that aim at perfect category separation, irrespective of overall category placement.

To investigate the role of recurrence, we also trained a control feedforward network, i.e., without recurrent and lateral and top-down connections.

All trained networks will be made available with the journal version of this paper.

#### *Predicting brain activity from DNN activations*

To compare the representations in our networks to the brain's representation, we apply a similar RSA approach as when comparing semantic GUSE embedding or category spaces with brain representations in experiment 1. First, RDMs for all images in the NSD dataset are computed in each layer and timestep of the network. Second, correlations between DNN and brain RDMs are computed in a searchlight fashion. The analysis at each searchlight location can be conducted either for a given layer and timestep of the DNN, or for the DNN as a whole using a fitting procedure.

To quantify how well layer L at timestep T predicts brain activity, we computed the correlation between the RDM for layer L at timestep T and the brain data RDM at each searchlight location (computed as described in *Information-based brain mapping*).

To quantify how well the network *as a whole* can predict brain data, we fit the RDMs of each layer and timestep of the RCNN and obtained a set of non-negative weights (one weight for each layer and timestep RDM), to best predict the brain representational geometry for that searchlight location. This non-negative least-squares fitting procedure is performed on multiple splits of the fMRI responses, for each participant independently, where on each split of 100 independent conditions, 70 images are chosen to train the weights, and 30 act as a test set. These weights are learnt on the training images and are then applied to the layer RDMs for the independent test set of 30 images to predict, for each searchlight sphere, the measured brain RDM. Depending on the total number of conditions shown to the NSD participants, this procedure is repeated until the sets of 100 image splits are exhausted (for the participant with fewer fMRI sessions, this resulted in 54 iterations of the nnls prediction procedure, and 100 iterations for the participants that completed all sessions of the NSD experiment). The averaged Pearson correlation across fitting iterations is reported.

### **Acknowledgements**

The authors acknowledge support by SNF grant n.203018 (Doerig), the ERC stg grant 101039524 TIME (Kietzmann), an ERC stg grant 759432 START (Charest), a Courtois Chair in computational neuroscience (Charest), and an NSERC Discovery grant (Charest). Collection of the NSD dataset was supported by NSF IIS-1822683 (Kay) and NSF IIS-1822929 (Naselaris).

### **Code and data availability**

The Natural Scenes Dataset is available at <http://naturalscenesdataset.org>. Code for the analyses reported here will be available upon publication of the manuscript.

## References

1. Ungerleider, L. G., Mishkin, L. Two cortical visual systems. in *Analysis of visual behavior* (ed. Goodale, M., Ingle, D. J., Mansfield, R. J. W.) (MIT Press, 1982).
2. Goodale, M. A. & Milner, A. D. Separate visual pathways for perception and action. *Trends Neurosci.* **15**, 20–25 (1992).
3. Ungerleider, L. G. & Haxby, J. V. ‘What’ and ‘Where’ in the human brain. *Curr. Opin. Neurobiol.* **4**, 157–165 (1994).
4. Hung, C. P., Kreiman, G., Poggio, T. & DiCarlo, J. J. Fast Readout of Object Identity from Macaque Inferior Temporal Cortex. *Science* **310**, 863–866 (2005).
5. DiCarlo, J. J., Zoccolan, D. & Rust, N. C. How Does the Brain Solve Visual Object Recognition? *Neuron* **73**, 415–434 (2012).
6. Kar, K. & DiCarlo, J. J. Fast Recurrent Processing via Ventrolateral Prefrontal Cortex Is Needed by the Primate Ventral Stream for Robust Core Visual Object Recognition. *Neuron* **109**, 164–176.e5 (2021).
7. Ito, M., Tamura, H., Fujita, I. & Tanaka, K. Size and position invariance of neuronal responses in monkey inferotemporal cortex. *J. Neurophysiol.* **73**, 218–226 (1995).
8. Hikosaka, K. Tolerances of responses to visual patterns in neurons of the posterior inferotemporal cortex in the macaque against changing stimulus size and orientation, and deleting patterns. *Behav. Brain Res.* **100**, 67–76 (1999).
9. Rust, N. C. & DiCarlo, J. J. Selectivity and Tolerance (‘Invariance’) Both Increase as Visual Information Propagates from Cortical Area V4 to IT. *Journal of Neuroscience* **30**, 12978–12995 (2010).
10. Haxby, J. V. *et al.* Distributed and Overlapping Representations of Faces and Objects in Ventral Temporal Cortex. *Science* **293**, 2425–2430 (2001).
11. Kiani, R., Esteky, H., Mirpour, K. & Tanaka, K. Object category structure in response patterns of neuronal population in monkey inferior temporal cortex. *J. Neurophysiol.* **97**, 4296–309 (2007).
12. Kriegeskorte, N. *et al.* Matching categorical object representations in inferior temporal cortex of man and monkey. *Neuron* **60**, 1126–1141 (2008).
13. Bonner, M. F. & Epstein, R. A. Object representations in the human brain reflect the co-occurrence statistics of vision and language. *Nat. Commun.* **12**, 4081 (2021).
14. Cichy, R. M., Khosla, A., Pantazis, D., Torralba, A. & Oliva, A. Comparison of deep neural networks to spatio-temporal cortical dynamics of human visual object recognition reveals hierarchical correspondence. *Sci. Rep.* **6**, 27755 (2016).
15. Horikawa, T. & Kamitani, Y. Generic decoding of seen and imagined objects using hierarchical visual features. *Nat. Commun.* **8**, 15037 (2017).
16. Cichy, R. M., Kriegeskorte, N., Jozwik, K. M., van den Bosch, J. J. F. & Charest, I. The spatiotemporal neural dynamics underlying perceived similarity for real-world objects. *Neuroimage* **194**, 12–24 (2019).
17. Hebart, M. N. *et al.* THINGS: A database of 1,854 object concepts and more than 26,000 naturalistic object images. *PLoS One* **14**, e0223792 (2019).
18. Kanwisher, N. Functional specificity in the human brain: a window into the functional architecture of the mind. *Proc. Natl. Acad. Sci. U. S. A.* **107**, 11163–11170 (2010).
19. Konkle, T. & Oliva, A. A Real-World Size Organization of Object Responses in Occipitotemporal Cortex. *Neuron* **74**, 1114–1124 (6/2012).
20. Bao, P., She, L., McGill, M. & Tsao, D. Y. A map of object space in primate inferotemporal cortex. *Nature* **583**, 103–108 (2020).
21. Krizhevsky, A., Sutskever, I. & Hinton, G. E. ImageNet Classification with Deep Convolutional Neural Networks. in *Advances in Neural Information Processing Systems 25* (eds. Pereira, F., Burges, C. J. C., Bottou, L. & Weinberger, K. Q.) 1097–1105 (Curran Associates, Inc., 2012).
22. Simonyan, K. & Zisserman, A. Very Deep Convolutional Networks for Large-Scale Image

Recognition. *arXiv [cs.CV]* (2014).

23. Kriegeskorte, N. Deep Neural Networks: A New Framework for Modeling Biological Vision and Brain Information Processing. *Annual Review of Vision Science* **1**, 417–446 (2015).
24. Richards, B. A. *et al.* A deep learning framework for neuroscience. *Nat. Neurosci.* **22**, 1761–1770 (2019).
25. Kriegeskorte, N. & Douglas, P. K. Cognitive computational neuroscience. *Nat. Neurosci.* **21**, 1148–1160 (2018).
26. Yamins, D. L. K. *et al.* Performance-optimized hierarchical models predict neural responses in higher visual cortex. *Proceedings of the National Academy of Sciences* (2014).
27. Cadieu, C. F. *et al.* Deep Neural Networks Rival the Representation of Primate IT Cortex for Core Visual Object Recognition. *arXiv preprint arXiv:1406.3284* (2014).
28. Khaligh-Razavi, S.-M. & Kriegeskorte, N. Deep Supervised, but Not Unsupervised, Models May Explain IT Cortical Representation. *PLoS Comput. Biol.* **10**, e1003915 (2014).
29. Kietzmann, T. C. *et al.* Recurrence is required to capture the representational dynamics of the human visual system. *Proc. Natl. Acad. Sci. U. S. A.* **116**, 21854–21863 (2019).
30. Güçlü, U. & van Gerven, M. A. J. Deep Neural Networks Reveal a Gradient in the Complexity of Neural Representations across the Ventral Stream. *J. Neurosci.* **35**, 10005–10014 (2015).
31. Doerig, A. *et al.* The neuroconnectionist research programme. *arXiv [q-bio.NC]* (2022).
32. Brandman, T. & Peelen, M. V. Interaction between Scene and Object Processing Revealed by Human fMRI and MEG Decoding. *J. Neurosci.* **37**, 7700–7710 (2017).
33. Miller, C. T. *et al.* Natural behavior is the language of the brain. *Curr. Biol.* **32**, R482–R493 (2022).
34. Mikolov, T., Chen, K., Corrado, G. & Dean, J. Efficient Estimation of Word Representations in Vector Space. *arXiv [cs.CL]* (2013).
35. Pennington, J., Socher, R. & Manning, C. GloVe: Global Vectors for Word Representation. in *Proceedings of the 2014 Conference on Empirical Methods in Natural Language Processing (EMNLP)* 1532–1543 (Association for Computational Linguistics, 2014).
36. Cer, D. *et al.* Universal Sentence Encoder for English. in *Proceedings of the 2018 Conference on Empirical Methods in Natural Language Processing: System Demonstrations* 169–174 (Association for Computational Linguistics, 2018).
37. Devlin, J., Chang, M.-W., Lee, K. & Toutanova, K. BERT: Pre-training of Deep Bidirectional Transformers for Language Understanding. *arXiv [cs.CL]* (2018).
38. Arora, S., Liang, Y. & Ma, T. A simple but tough-to-beat baseline for sentence embeddings. in *International Conference on Learning Representations* (2017).
39. Allen, E. J. *et al.* A massive 7T fMRI dataset to bridge cognitive neuroscience and artificial intelligence. *Nat. Neurosci.* **25**, 116–126 (2022).
40. Olshausen, B. A. & Field, D. J. Emergence of simple-cell receptive field properties by learning a sparse code for natural images. *Nature* **381**, 607–609 (1996).
41. Portilla & Simoncelli. A Parametric Texture Model Based on Joint Statistics of Complex Wavelet Coefficients. in *International conference on computer vision* (Kluwer Academic Publishers, 2000).
42. Lin, T.-Y. *et al.* Microsoft COCO: Common Objects in Context. *arXiv [cs.CV]* (2014).
43. Chen, X. *et al.* Microsoft COCO Captions: Data Collection and Evaluation Server. *arXiv [cs.CV]* (2015).
44. Kriegeskorte, N., Mur, M. & Bandettini, P. Representational similarity analysis - connecting the branches of systems neuroscience. *Front. Syst. Neurosci.* **2**, 4 (2008).
45. Kriegeskorte, N. & Kievit, R. A. Representational geometry: integrating cognition, computation, and the brain. *Trends Cogn. Sci.* **17**, 401–412 (8/2013).
46. Nili, H. *et al.* A Toolbox for Representational Similarity Analysis. *PLoS Comput. Biol.* **10**, e1003553 (2014).
47. Kay, K. N., Naselaris, T., Prenger, R. J. & Gallant, J. L. Identifying natural images from human brain activity. *Nature* **452**, 352–5 (2008).

48. Xu, K. *et al.* Show, Attend and Tell: Neural Image Caption Generation with Visual Attention. *arXiv [cs.LG]* (2015).
49. He, S. *et al.* Image Captioning through Image Transformer. *arXiv [cs.CV]* (2020).
50. Mehrer, J., Spoerer, C. J., Jones, E. C., Kriegeskorte, N. & Kietzmann, T. C. An ecologically motivated image dataset for deep learning yields better models of human vision. *Proc. Natl. Acad. Sci. U. S. A.* **118**, (2021).
51. DiCarlo, J. J. & Cox, D. D. Untangling invariant object recognition. *Trends Cogn. Sci.* **11**, 333–341 (2007).
52. Radford, A. *et al.* Learning Transferable Visual Models From Natural Language Supervision. *arXiv [cs.CV]* (2021).
53. Dado, T. *et al.* Hyperrealistic neural decoding for reconstructing faces from fMRI activations via the GAN latent space. *Sci. Rep.* **12**, 141 (2022).
54. Défossez, A., Caucheteux, C., Rapin, J., Kabeli, O. & King, J.-R. Decoding speech from non-invasive brain recordings. *arXiv [eess.AS]* (2022).
55. Huang, W. *et al.* A dual-channel language decoding from brain activity with progressive transfer training. *Hum. Brain Mapp.* **42**, 5089–5100 (2021).
56. Friston, K. The free-energy principle: a unified brain theory? *Nat. Rev. Neurosci.* **11**, 127–138 (2010).
57. Knill, D. C. & Pouget, A. The Bayesian brain: the role of uncertainty in neural coding and computation. *Trends Neurosci.* **27**, 712–719 (2004).
58. Hochstein, S. & Ahissar, M. View from the top: hierarchies and reverse hierarchies in the visual system. *Neuron* **36**, 791–804 (2002).
59. Ahissar, M. & Hochstein, S. The reverse hierarchy theory of visual perceptual learning. *Trends Cogn. Sci.* **8**, 457–464 (2004).
60. Rogers, T. T. & Lambon Ralph, M. A. Semantic tiles or hub-and-spokes? *Trends Cogn. Sci.* **26**, 189–190 (2022).
61. Huth, A. G., de Heer, W. A., Griffiths, T. L., Theunissen, F. E. & Gallant, J. L. Natural speech reveals the semantic maps that tile human cerebral cortex. *Nature* **532**, 453–458 (2016).
62. Güçlü, U. & van Gerven, M. A. J. Semantic vector space models predict neural responses to complex visual stimuli. *arXiv [q-bio.NC]* (2015).
63. Zhang, Y., Han, K., Worth, R. & Liu, Z. Connecting concepts in the brain by mapping cortical representations of semantic relations. *Nat. Commun.* **11**, 1877 (2020).
64. Popham, S. F. *et al.* Visual and linguistic semantic representations are aligned at the border of human visual cortex. *Nat. Neurosci.* **24**, 1628–1636 (2021).
65. Müller, R., Kornblith, S. & Hinton, G. When Does Label Smoothing Help? *arXiv [cs.LG]* (2019).
66. Wang, A. Y., Tarr, M. J. & Wehbe, L. Image Embeddings Informed by Natural Language Significantly Improve Predictions and Understanding of Human Higher-level Visual Cortex. in *Conference on Cognitive Computational Neuroscience*.
67. Muttenthaler, L. & Hebart, M. N. THINGSvision: A Python Toolbox for Streamlining the Extraction of Activations From Deep Neural Networks. *Front. Neuroinform.* **15**, 679838 (2021).
68. Elmoznino, E. & Bonner, M. F. High-performing neural network models of visual cortex benefit from high latent dimensionality. *bioRxiv* 2022.07.13.499969 (2022) doi:10.1101/2022.07.13.499969.
69. Kriegeskorte, N. & Douglas, P. K. Interpreting encoding and decoding models. *Curr. Opin. Neurobiol.* **55**, 167–179 (2019).
70. Diedrichsen, J. Representational models and the feature fallacy. in *The Cognitive Neurosciences*. (The MIT Press, 2020).
71. Ralph, M. A. L., Jefferies, E., Patterson, K. & Rogers, T. T. The neural and computational bases of semantic cognition. *Nat. Rev. Neurosci.* **18**, 42–55 (2017).
72. Charest, I., Kievit, R. A., Schmitz, T. W., Deca, D. & Kriegeskorte, N. Unique semantic space in the brain of each beholder predicts perceived similarity. *Proceedings of the National Academy of*

*Sciences* **111**, 14565–14570 (2014).

- 73. Kriegeskorte, N., Goebel, R. & Bandettini, P. A. Information-based functional brain mapping. *Proc. Natl. Acad. Sci. U. S. A.* **103**, 3863–3868 (2006).
- 74. Haynes, J. D. & Rees, G. Predicting the stream of consciousness from activity in human visual cortex. *Curr. Biol.* **15**, 1301–7 (2005).

## Supplementary Materials

### Supplementary figure 1

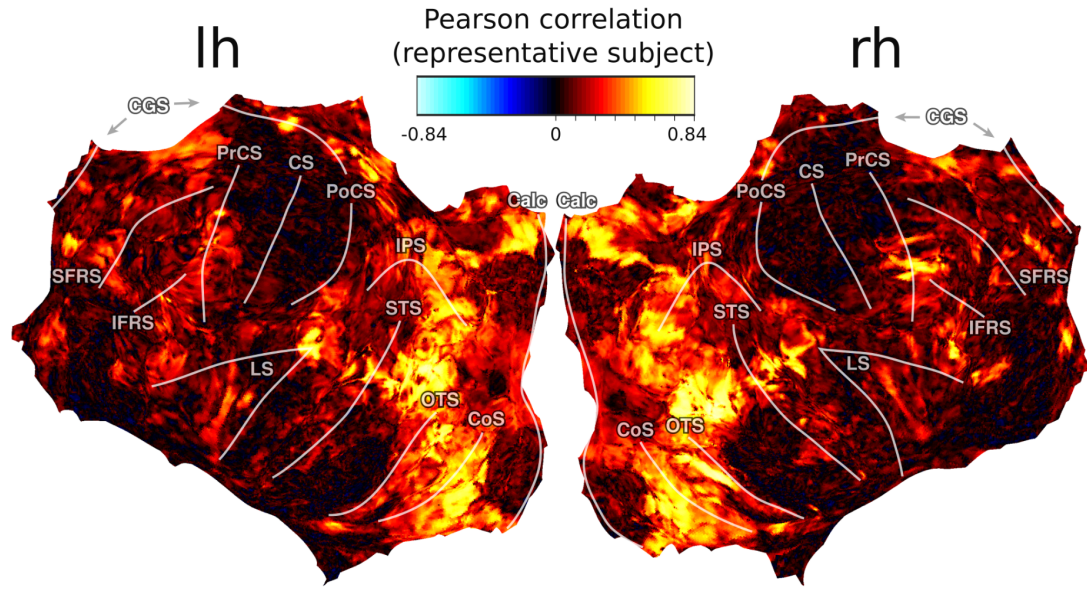


**Figure S1. Predicting voxel-wise responses using sentence embeddings.** Complementary to our representational similarity analysis performed with a searchlight procedure, we tested whether GUSE could be used to perform voxel-wise encoding modelling. This was done using cross-validated fractional ridge regression, using the common 1000 images as a test set (the images shared across the 8 subjects), and training on the subject-specific images (the images shown to each individual subject). Linear weights were learned, using the training set, to map between the 512 dimensional embedding space (from the images' sentence captions) and the fMRI beta responses (averaged across the three repetitions). These linear weights were then applied onto the embedding space of the test set, to predict the beta responses for that test set. Shown is the Pearson correlation between the predicted beta responses, and the actual observed beta responses for this test set. The prediction is displayed on a cortical flat-map, and the heatmap reveals very accurate predictions, bilaterally, in regions of the visual ventral stream and extended regions of the medial temporal lobe, parietal cortex, and the pre-frontal cortex. The network of brain regions revealed by this voxel-wise encoding procedure is very similar to that obtained with our RSA searchlight mapping procedure. Altogether, this is an additional demonstration of the accuracy that sentence embeddings provide as a representational space predicting brain activity in the visual cortex.

## Supplementary figure 2

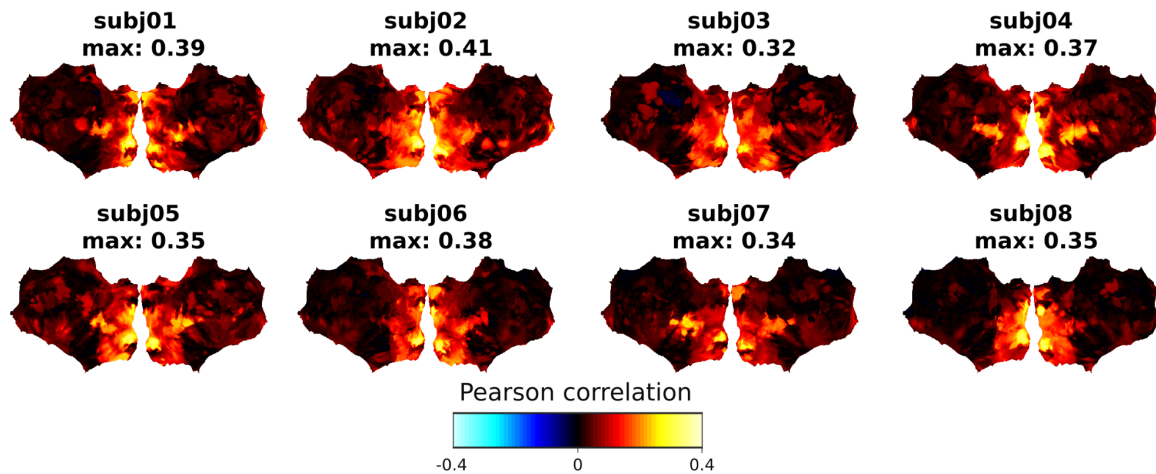


**Figure S2. RCNN model fit for individual subjects.** We performed a cross-validated non-negative least squares RSA searchlight fit comparing our RCNN model trained on semantics with brain derived RDMs in the local searchlights. Results show that the RCNN model explains brain activity across the whole of the visual ventral stream, explaining computations from early visual cortex (EVC) until high-level semantic representations.

### Supplementary Figure 3

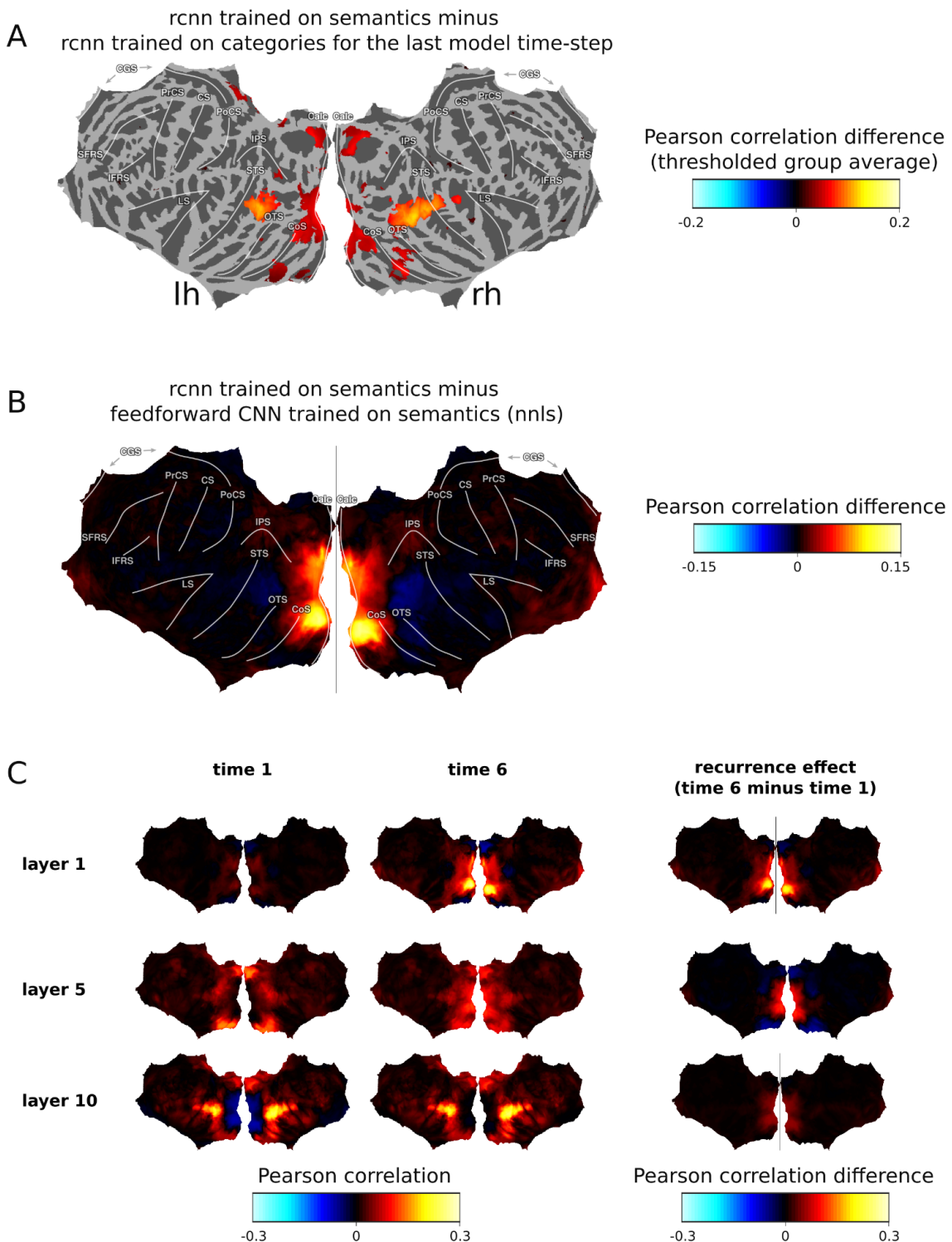


**Figure S3. Isolating the effect of a semantic objective and of recurrent processing.** A) *Semantically trained vs. category trained RCNN.* Searchlight maps of Pearson correlation between brain- and RCNN-derived RDMs. The last layer and timestep of the semantically trained RCNN explains brain activity better than the last layer and timestep of the category-trained RCNN both in high-level

semantic areas and low-level EVC. B) *Recurrent semantically trained RCNN vs. feedforward semantically trained RCNN*. To visualise the impact of recurrence across the network's layers, and to avoid the problem that the feedforward and recurrent models have different number of timesteps, this analysis combines all network layers using non-negative least-squares averaged across subjects. Recurrence strongly improves the fit to EVC, but does not strongly change the fit to higher order regions. C) *Effect of recurrence at different depths*. Searchlight maps of Pearson correlation between brain- and RCNN-derived RDMs derived from the semantically trained RCNN at different layers (rows) and timesteps (columns 1&2). Column 3 shows the difference between the last and the first timestep, highlighting the outcome of recurrent processing. Recurrence strongly improves the fit to EVC for layer 1, less so for layer 5 and only very mildly for layer 10. Together, these results suggest that recurrence is essential in explaining why semantically trained networks better explain EVC than category-trained networks.